

Relativistic photoionization cross sections for C II

Sultana N. Nahar

Department of Astronomy, The Ohio State University, Columbus, Ohio 43210

(October 31, 2018)

Abstract

High resolution measurements of photoionization cross sections for atomic ions are now being made on synchrotron radiation sources. The recent measurements by Kjeldsen et al. (1999) showed good agreement between the observed resonance features and the theoretical calculations in the close coupling approximation (Nahar 1995). However, there were several observed resonances that were missing in the theoretical predictions. The earlier theoretical calculation was carried out in LS coupling where the relativistic effects were not included. Present work reports photoionization cross sections including the relativistic effects in Breit-Pauli R-matrix (BPRM) approximation. The configuration interaction eigenfunction expansion for the core ion C III consists of 20 fine structure levels dominated by the configurations from $1s^2 2s^2$ to $1s^2 2s 3d$. Detailed features in the calculated cross sections exhibit the missing resonances due to fine structure. The present results benchmark the accuracy of BPRM photoionization cross sections as needed for recent and ongoing experiments.

PACS number(s): 32.80.Fb

Although a large number of theoretical calculations for photoionization cross sections have been carried out, the theoretical data have not yet been benchmarked against the new generation of high-resolution experiments. We refer in particular the calculations using the close coupling R-matrix method for extensively utilized in the Opacity Project [3] and similar works that accurately considers the numerous autoionizing resonances in the cross sections along overlapping Rydberg series. Most of the vast amount of photoionization data computed under the Opacity Project (OP), Iron Project (IP) [4] and other works, as estimated to be accurate to 10-20%. However, no detailed comparisons with experiments have been possible since photoionization cross sections were not measured with equally detailed features. Resonances can now be finely resolved in recent experiments being carried out with synchrotron radiation sources in Aarhus [1], Berkely (e.g. [?]), and Paris (e.g. [6]). The test of benchmarking the theoretical calculations with experiments is therefore of considerable current importance. Furthermore, the quality of experimental work is such as to clearly delineate the fine structure, necessitating the inclusion of relativistic effects in an *ab initio* manner. In this *Communication* we present and benchmark the first theoretical results with recent experimental data.

Carbon is one of the most cosmically abundant elements and C II is an important ion in astrophysical sources such as the interstellar medium. Study of accurate features of C II is of considerable interest and important for accurate spectral analysis. In their merged ion-photon beam experiment, Kjeldsen et al. [1] measured the first detailed photoionization cross sections (σ_{PI}) of C II with high accuracy. With the synchrotron radiation from an undulator, their measurement exhibited highly resolved features of autoionizing resonances in the cross sections. The features agreed very well with the results from close coupling approximation using the R-matrix method [2]. However, the theoretical calculations did not include the relativistic effects and therefore did not predict the observed fine structure features.

The Opacity Project work did not include the fine structure. The motivation for the present work is to study the fine structure effects in relation to the observed features using

the Breit-Pauli R-matrix (BPRM) method [7,4,8]. The method has been extended to a self-consistent treatment of photoionization cross sections and electron ion recombination (e.g [9]) and benchmarked for the total recombination cross sections in a unified treatment by comparing with measured recombination spectra [9,10]. The recombination cross sections require total contributions of photoionization cross sections of all bound levels. On the contrary, present work focuses on the features of photoionization cross sections of single levels of ground configurations, $2s^22p$, of C II, and compares with the recent measured cross sections.

The theoretical calculations for the photoionization cross sections (σ_{PI}) are carried out in the close coupling (CC) approximation using Breit-Pauli R-matrix method in intermediate coupling. Photoionization of the ion is described in terms of the eigenfunction expansion over coupled levels of the residual ('core' or 'target') ion. The wavefunction of the (N+1)-electron ion is represented by the level wavefunctions of the N-electron core multiplied by the wavefunction of the outer electron as follows:

$$\Psi(E) = A \sum_i \chi_i \theta_i + \sum_j c_j \Phi_j, \quad (0.1)$$

χ_i is the target wavefunction in a specific level $J_i \pi_i$ and θ_i is the wavefunction for the (N+1)-th electron in a channel labeled as $S_i L_i (J_i) \pi_i k_i^2 \ell_i (J \pi)$; k_i^2 being its incident kinetic energy. Φ_j 's are the correlation functions of the (N+1)-electron system that account for short range correlation and the orthogonality between the continuum and the bound orbitals.

The BP Hamiltonian, as employed in the IP work [4], is

$$H_{N+1}^{\text{BP}} = H_{N+1} + H_{N+1}^{\text{mass}} + H_{N+1}^{\text{Dar}} + H_{N+1}^{\text{so}}, \quad (0.2)$$

where H_{N+1} is the nonrelativistic Hamiltonian,

$$H_{N+1} = \sum_{i=1}^{N+1} \left\{ -\nabla_i^2 - \frac{2Z}{r_i} + \sum_{j>i}^{N+1} \frac{2}{r_{ij}} \right\}, \quad (0.3)$$

and the additional terms are the one-body mass correction term, the Darwin term and the spin-orbit interaction term respectively.

Present wavefunction for C II is expressed by an 20-level expansion of the core ion, C III, with configurations, $2s^2$, $2s2p$, $2p^2$, $2s3s$, $2s3p$, $2s3d$, while the K-shell remains closed (Table I). The core wavefunction was obtained from atomic structure calculations with Thomas-Fermi potential using the code SUPERSTRUCTURE [11]. The spectroscopic and correlation configurations and the scaling parameters in the Thomas-Fermi potential are given in Table I. The correlation term in Eq. (1) considers all possible (N+1)-electron configurations formed from the maximum occupancies in the orbitals as $2p^3$, $3s^2$, $3p^2$, $3d^2$, $4s^2$, $4p^2$.

The computations of σ_{PI} are carried out using the package of BPRM codes [8] from the Iron Project. The cross sections are computed with a very fine energy mesh in order to delineate the detailed resonance structures as observed in the experiments. It is a computationally demanding procedure because of repeated computations with exceedingly fine energy bins to search and resolve the resonances. Many resonances are sharp and narrow, and can not be detected individually in the experiment. They are convolved with a Gaussian function of FWHM equal to the energy bandwidth of the monochrometer of the experiment.

The calculated photoionization cross sections (σ_{PI}) of levels $^2P_{1/2}^o$ and $^2P_{3/2}^o$ of ground configuration $2s^22p$ of C II are presented in Fig. 1. Inclusion of relativistic effects in the BPRM approximation introduces more Rydberg series of resonances in the cross sections belonging to the increased number of core thresholds by fine structure splitting.

The BPRM cross sections are presented in the bottom panel of Fig. 1 where σ_{PI} of $^2P_{1/2}^o$ level is shown as the solid curve, and of $^2P_{3/2}^o$ level as the dotted curve. Both cross sections have many overlapping resonances. They are compared with the photoionization cross sections of the $^2P^o$ ground state of C II in LS coupling (Fig. 1a, upper panel). The 12 C III core states in LS coupling correspond to 20 fine structure levels. The additional thresholds as well as resonances that are not allowed in LS coupling but are allowed in intermediate coupling (IC) have resulted in more extensive resonances in the BPRM σ_{PI} . For example, photoionization of $2s^22p(^2P^o)$ is allowed to 2S and 2D channels only, not to 2P in LS coupling. However, with the IC the (e+ion) symmetry 2P is enabled since $^2P_{1/2}$ can

mix with ${}^2S_{1/2}$, and ${}^2P_{3/2}$ can mix with ${}^2D_{3/2}$. The first series of resonances $2s2p({}^3P^o)np({}^2P)$ with $n = 4, 5, \dots$ (denoted as R1 series in Fig. 1b) appearing in BPRM calculations are not seen in LS coupling (Fig. 1a). The next two series of resonances, $2s2p({}^3P^o)np({}^2D, {}^2S)$ (denoted as R2 and R3 series) are common to both LS and BPRM. The 4th series of resonances, which could be identified as the combination of $2s2p({}^1P^o)np({}^2D, {}^2P, {}^2S)$, are also common (except for the 2P component) although they are very weak in LS coupling calculations partially due to coarser energy mesh. Identification of this series differs from Kjeldsen et al. [1] who assigned a different series with the same identification. This series was not observed in their measurement. Additional series of resonances are introduced starting from the fourth complex which overlap with the others. Small shift in energy positions of the resonances, seen in the upper and lower panels of Fig. 1, is due to statistical averaging of LS energy terms over their fine structure components.

The BPRM photoionization cross sections are compared with the measured cross sections by Kjeldson et al. (1999) after convolving the calculated resonances with a Gaussian distribution function with a FWHM of 35 meV, the monochrometer bandwidth of the experiment. The calculated ionization energy for the ${}^2P_{1/2}^o$ ground level is 1.7885 eV compared to the measured energy of 1.7921 eV, and for ${}^2P_{3/2}^o$ level it is 1.78793 eV compared to the measured one of 1.7916 eV. The calculated cross sections have been slightly shifted to the measured ionization thresholds to compare with the experimentally measured σ_{PI} in Fig. 2.

Fig 2a, presents the total detailed calculated cross sections of the levels ${}^2P_{1/2,3/2}^o$ (solid and dotted curves respectively) while Fig. 2b presents the convolved σ_{PI} on the eV scale. The measured cross sections [1] are presented in Fig. 2c. Very good agreement is seen in general in resonance features between the calculations (Fig. 2b) and the measurements (Fig. 2c). The resonance peaks are also in good agreement in the first three resonance complexes. However, some differences may be noticed for the higher complexes. The peaks of some calculated resonances at higher energies are higher than the measured ones. These peaks are not expected to be damped by dielectronic recombination or the radiative decays of the excited core thresholds; the decay rates ($\approx 10^8, 10^9 \text{ sec}^{-1}$) are several orders of magnitude

lower than typical autoionization rate of $10^{13-14} \text{ sec}^{-1}$. These peaks were checked with inclusion of radiation damping effect with no significant reduction. However, several other reasons can explain the differences. The measured convolved cross sections are not usually purely Gaussian as assumed in the calculated cross sections. The same FWHM may not remain constant with energies and the peaks may be lowered with a larger bandwidth. The detailed resonances can be convolved with varied bandwidths to conform to the observed features. Also, the cross sections might be further resolved with a finer energy mesh to reduce the differences in the high energy peaks. It may be mentioned that as resonances get narrower with energy approaching to the convergent threshold, the monochromator requires a narrower bandwidth for finer resolution. To see the structures at higher energies near the highest threshold, the resonances beyond 30.2 eV are convolved with a narrower FWHM, and hence seem sharper than the measured cross sections. Fig. 2d presents the convolved cross sections of excited $2s2p^2(^4P_J)$ levels in a smaller resonant energy region, from 24.2 eV to about 25.5 eV, as discussed below.

Photoionization cross sections of the three fine structure levels, $J = 1/2, 3/2,$ and $5/2,$ of the first excited state $2s2p^2(^4P)$ of C II are also presented. Kjeldsen et al. [1] found a few resonances of $2s2pnd$ ($n=7,8,..$) series from photoionization of 4P state in the near threshold region of ground state of C II. These resonances belong to the allowed transitions in IC among levels of $2s2p^2(^4P_J)$ and $2s2pnd(^2P_J^o, ^2D_J^o)$, that are forbidden in LS coupling. Fig. 3a (top panel) presenting σ_{PI} of 4P state in LS coupling, shows that there are no resonances below the threshold at 1.872 Ry photoionizing to $2s2p(^3P^o)$ state of C III. However, extensive narrow resonances can be seen below this threshold with almost no background in the photoionization cross sections of the fine structure levels $^4P_{1/2,3/2,5/2}$, shown separately as solid, dotted and dashed curves in Fig. 3. The ionization thresholds for these levels lie at about 1.4 Ry (pointed by arrow in the figure) and each level exhibits presence of a near threshold resonance. As we are interested in the overlapping energy region with the ground state of C II, the resonances of the levels $J = 1/2, 3/2, 5/2$ are resolved with a much finer energy mesh from ≈ 1.75 Ry to about 1.87 Ry. These narrow resonances are convolved with

the same monochrometer bandwidth of 35 meV and are presented in Fig. 2d for comparison with the measured cross sections. The first three of the convolved peaks were identified by Kjeldsen et al. [1] as they were observed in the experiment (Fig. 2c), indicating that there was a mixture of states $^2P^o$ and 4P in their C II beam in the low energy region. The convolved resonance peaks are lower, except for the first one, than the observed ones. Further resolution of the resonances could conceivably have improved the agreement with the measured ones.

We have demonstrated that the theoretical fine structure photoionization cross sections account for nearly all experimentally observed features. The relativistic BPRM photoionization cross sections of the ground state and the first excited state of C II reveal the fine structure observed in experiments, but not obtained in the non-relativistic LS coupling calculation. Very good agreement is found between the BPRM cross sections and the measured cross sections [1]. Convolution of the detailed resonances with a monochrometer bandwidth may result in some variations of peaks depending on the bandwidth, choice of energy distribution function and resolution of resonances.

Similar to the experimental work by Kjeldsen et al. [1], Phaneuf et al. [5] are currently measuring photoionization cross sections of C II at a different set-up at ALS (Advance Light Source). However, the resolution at ALS is much higher (the estimated monochromite bandwidth is about 7 meV compared to 35 meV by Kjeldsen et al.). The cross sections from the present work are available electronically for comparison with other experiments.

This work was partially supported by the National Science Foundation and the NASA Astrophysical Theory Program. The computational work was carried out at the Ohio Supercomputer Center.

REFERENCES

- [1] H. Kjeldsen, F. Folkmann, J.E. Hensen, H. Knudsen, M.S. Rasmussen, J.B. West, T. Andersen, *Astrophys. J.* **524**, L143 (1999); (the experimental data were obtained through private communication).
- [2] S. N. Nahar, *Astrophys. J. Suppl.* **101**, 423 (1995).
- [3] *The Opacity Project 1 & 2*, compiled by the Opacity Project team (Institute of Physics, London, UK, 1995,1996).
- [4] D.G. Hummer, K.A. Berrington, W. Eissner, A.K. Pradhan, H.E. Saraph and J.A. Tully, *Astron. Astrophys.* **279**, 298 (1993).
- [5] R. Phaneuf, F. Schlachter et al. (private communication, 2001).
- [6] J.-M. Bizau et al., *Phys. Rev. Lett.* **84**, 435 (2000).
- [7] N.S. Scott and K.T. Taylor, *Comput. Phys. Commun.* **25**, 347 (1982); N.S. Scott and P.G. Burke, *J. Phys. B* **12**, 4299 (1980).
- [8] K.A. Berrington, W. Eissner, P.H. Norrington, *Comput. Phys. Commun.* **92**, 290 (1995).
- [9] H.L. Zhang, S.N. Nahar, and A.K. Pradhan, *Journal Of Physics B* **32**, 1459 (1999).
- [10] A.K. Pradhan, S.N. Nahar, and H.L. Zhang, *Astrophys. J. Lett* **549**, L265 (2001).
- [11] W. Eissner, M. Jones and N. Nussbaumer, *Comput. Phys. Commun.* **8**, 270 (1974).

FIGURES

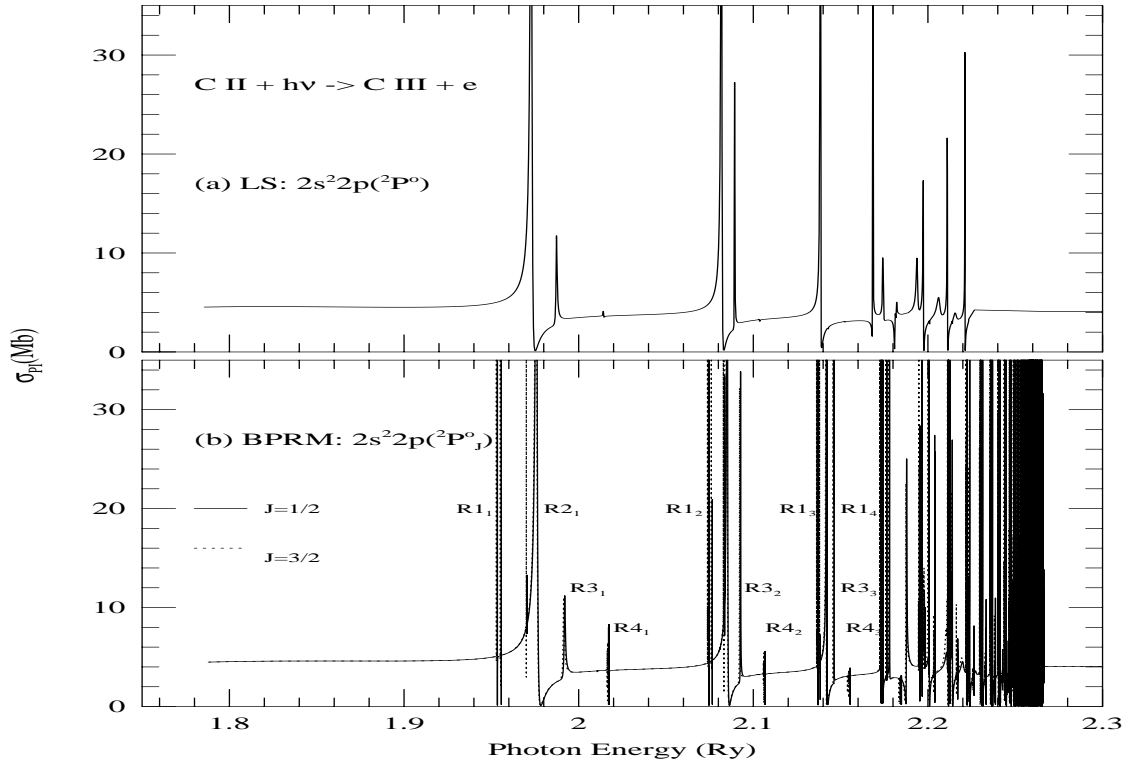


FIG. 1. Photoionization cross sections σ_{PI} of the (a) ground $2s^2 2p(^2P^o)$ state in LS coupling, and (b) levels $^2P^o_J$, where $J = 1/2$ (solid curve) and $3/2$ (dotted curve) in BPRM intermediate coupling, of ground configuration of C II.

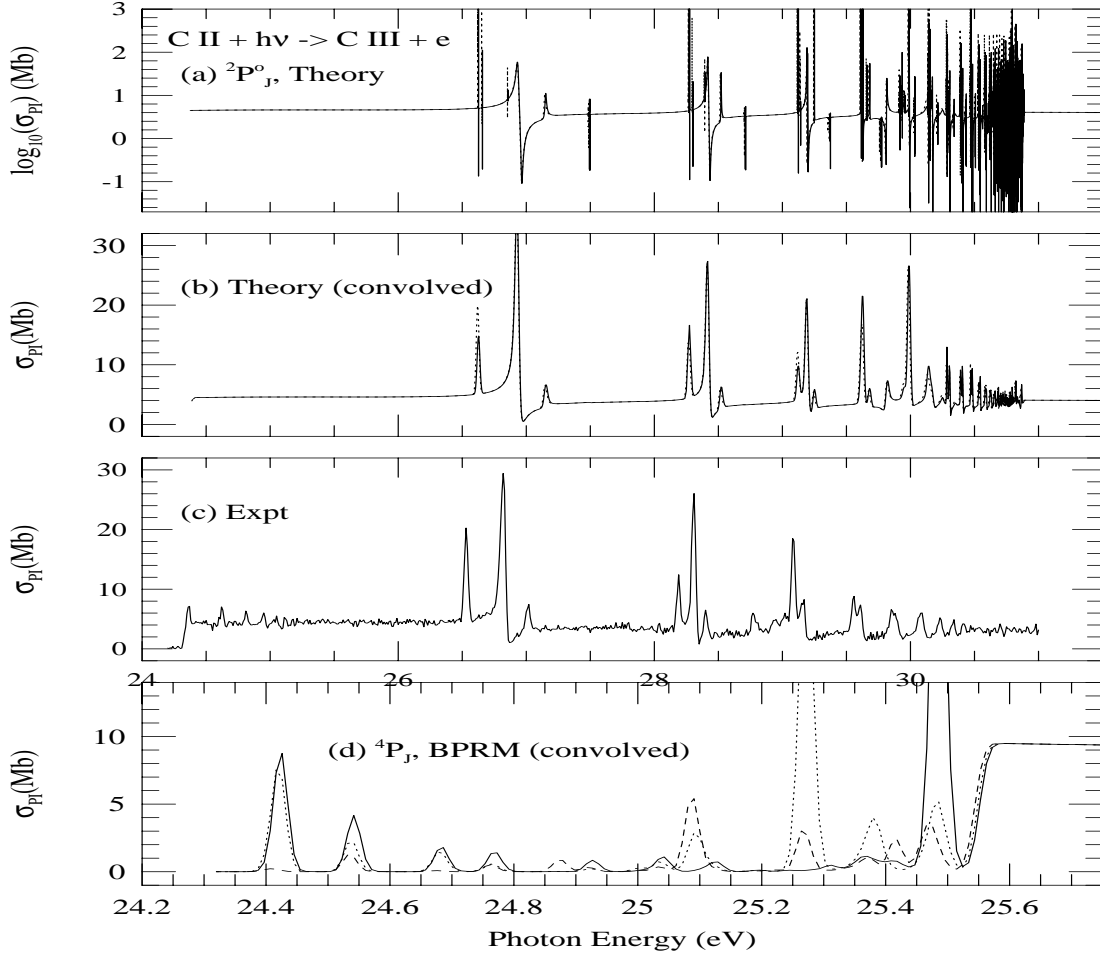


FIG. 2. Photoionization cross sections σ_{PI} of C II: (a) detailed with resonances of levels ${}^2P_{1/2}^o$ (solid) and ${}^2P_{3/2}^o$ (dotted) of ground configuration $1s^22s^22p$, (b) the same cross sections convolved with monochrometer bandwidth of the experiment, (c) experimentally measured cross sections; (d) convolved cross sections of excited levels $2s2p^2({}^4P_J)$, solid - $J=1/2$, dotted - $J=3/2$, dashed - $J=5/2$.

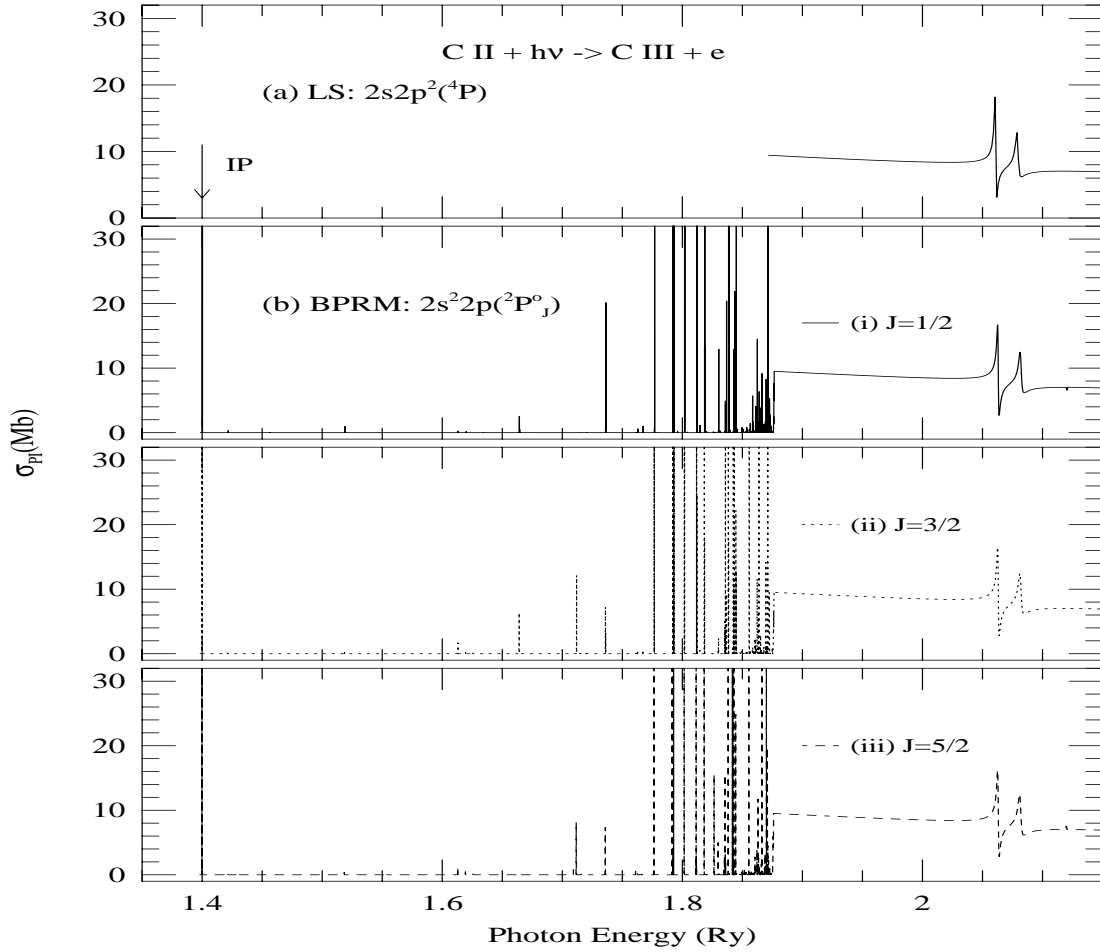


FIG. 3. Photoionization cross sections of the first excited $2s2p^2(^4P)$ state of C II: (a) in LS coupling, (b) of levels (i) $J=1/2$, (ii) $J=3/2$, and (iii) $J=5/2$ in BPRM approximation. Arrow points the ionization threshold for the fine structure levels.

TABLES

TABLE I. Energy Levels of C III in the eigenfunction expansion of C II. The list of spectroscopic and correlation configurations, and the scaling parameter (λ) for each orbital are given below the table.

	Level		E(Ry)
1	$2s^2$	1S_0	0.
2	$2s2p$	$^3P_2^o$	0.47793
3	$2s2p$	$^3P_1^o$	0.4774
4	$2s2p$	$^3P_0^o$	0.4772
5	$2s2p$	$^1P_1^o$	0.9327
6	$2p^2$	3P_2	1.2530
7	$2p^2$	3P_1	1.2526
8	$2p^2$	3P_0	1.2523
9	$2p^2$	1D_2	1.3293
10	$2p^2$	1S_0	1.6632
11	$2s3s$	3S_1	2.1708
12	$2s3s$	1S_0	2.2524
13	$2s3p$	$^1P_1^o$	2.3596
14	$2s3p$	$^3P_2^o$	2.3668
15	$2s3p$	$^3P_1^o$	2.3667
16	$2s3p$	$^3P_0^o$	2.3666
17	$2s3d$	3D_3	2.4606
18	$2s3d$	3D_2	2.4605
19	$2s3d$	3D_1	2.4605
20	$2s3d$	1D_2	2.5195

Spectroscopic: $2s^2, 2s2p, 2p^2, 2s3s, 2s3p, 2s3d$

Correlation: $2p3s, 2p3p, 2p3d, 3s3p, 3s3d, 2s4s, 2s4p, 4s4p$

λ : 1.42(1s), 1.4(2s), 1.125(2p), 1.(3s), 1(3p), 1(3d), 3.3(4s),
3(4p)
